RSC Advances

Check for updates

Cite this: *RSC Adv.*, 2017, **7**, 52001

Pentasaccharide resin glycosides with multidrug resistance reversal activities from the seeds of *Pharbitis nil*†

Jun Li,[ab] Wen-Qiong Wang,[ab] Shuai Tang,[ab] Wei-Bin Song,[ab] Min Huang[ab] and Li-Jiang Xuan [ID] *[ab]

Resin glycosides are novel P-glycoprotein inhibitors. In order to evaluate their multidrug resistance (MDR) reversal activities, we isolated seven new resin glycosides, pharbitins A–G (**1–7**) from the seeds of *Pharbitis nil*. Their chemical structures were determined by extensive application of high resolution 2D NMR techniques, HRESIMS and chemical methods. Compounds **1–4** and **6** were evaluated for their MDR reversal activities in KB/VCR, A549/T and K562/ADR cells. Among them, compound **2** showed moderate MDR reversal activity in KB/VCR cells, and increased the cytotoxicity of vincristine by 2.2-fold when incorporated at 25 μM. A structure–activity relationship study revealed that substituting Rha″ C-3 with a *trans*-cinnamoyl group improves the MDR reversal activity. Also, an intracellular Rh123 accumulation assay demonstrated that compound **2** could inhibit the function of P-gp.

Introduction

Resin glycosides are unusual amphipathic metabolites with structures including hydrophobic (fatty acid aglycone) and hydrophilic (oligosaccharide) moieties, which are mainly found in the family Convolvulaceae.[1] Resin glycosides exhibit various pharmacological activities, such as cytotoxicity, multidrug resistance (MDR) reversal, ionophoresis, and phytogrowth–inhibitory activities.[2–4] Because of their intriguing structures and varied activities, resin glycosides have attracted more attention in recent times. Moreover, as novel P-glycoprotein inhibitors, the resin glycosides from *Merremia hederacea* with MDR reversal activities have been investigated in our previous work.[5] However, considering the unclear structure–activity relationship (SAR) and pharmacological mechanism of the resin glycosides, we intend to isolate various analogues from the family Convolvulaceae, investigate their MDR reversal activities, and then proceed to establish their SAR and pharmacological mechanism.

Pharbitidis Semen, the seeds of *Pharbitis nil*, is a purgative crude drug widely grown in China and Japan.[6] So far, only four pure resin glycoside acids (pharbitic acids A–D) with an acyclic core have been reported from *P. nil*.[6–8] We report the isolation of

seven new resin glycosides pharbitins A–G (**1–7**) (Fig. 1) with macrolactone rings from the seeds of *P. nil*. According to their structures, the new compounds can be divided into two types: those possessing 18-membered rings (**1–5**), and compounds **6–7** with 19-membered rings. Among them, **2** showed moderate activity in MDR reversal against KB/VCR cells, and increased the cytotoxicity of vincristine by 2.2-fold when incorporated at 25 μM. Herein, we described the isolation, structural elucidation and MDR reversal activity evaluation of all isolates from the seeds of *P. nil*.

Results and discussion

Pharbitin A (**1**) was obtained as a colorless gum. The molecular formula was established as $C_{66}H_{104}O_{27}$ based on ^{13}C NMR data (Table 3) and HRESIMS ion at *m/z* 1351.6647 $[M + Na]^+$ (calcd for $C_{66}H_{104}O_{27}Na$, 1351.6657). Its IR spectrum exhibited absorptions of hydroxyl (3426 cm^{-1}), carbonyl (1724 cm^{-1}), and aromatic (1635 cm^{-1}) groups. The NMR spectra showed five anomeric signals $[\delta_H 4.90 (d, J = 7.5 Hz), \delta_H 5.12 (d, J = 7.6 Hz), \delta_H 5.59 (d, J = 1.8 Hz), \delta_H 5.85 (d, J = 1.8 Hz), \delta_H 6.29 (d, J = 1.8 Hz)]$ and $\delta_C 166.8, 173.7, 173.9, 176.3]$ and signals of long-chain fatty acids, which indicated that **1** was a resin glycoside.[9] The NMR data of **1** could be divided into two parts: resonances in the anomeric region and those representative of the aglycone moieties.

For the aglycone part, the ^1H NMR data of **1** (Table 1) exhibited two *trans*-coupled olefinic protons at $\delta_H 6.59 (d, J = 16.0 Hz)$ and $\delta_H 7.85 (d, J = 16.0 Hz)$ due to *trans*-cinnanoyl group (CA). The signals at $\delta_H 0.79 (t, J = 7.0 Hz)$ and $\delta_H 2.31 (m)$ due to the *n*-octanoyl group (Octa). Also a methyl triplet signal at

State Key Laboratory of Drug Research, Shanghai Institute of Meteria Medica, Chinese Academy of Sciences, 501 Haike Road, Shanghai 201201, People's Republic of China. E-mail: ljxuan@simm.ac.cn; Fax: +86-21-20231968; Tel: +86-21-20231968

University of Chinese Academy of Sciences, No. 19A Yuquan Road, Beijing 100049, People's Republic of China

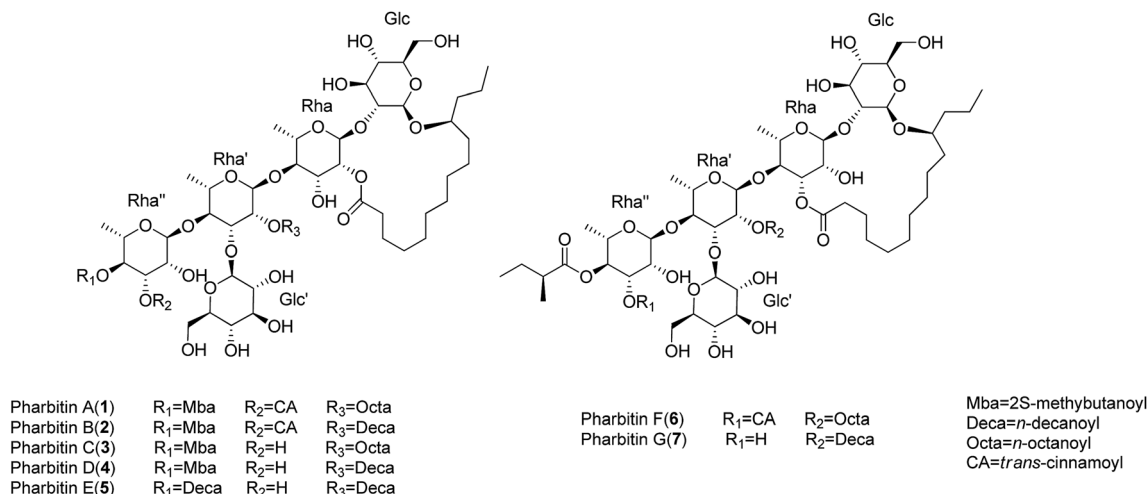† Electronic supplementary information (ESI) available. See DOI: 10.1039/c7ra09026a

Fig. 1   Chemical structures of compounds 1–7.

δ_H 0.82, a methyl doublet signal at δ_H 1.14 and a methine multiplet signal at δ_H 2.49 due to 2-methylbutanoyl moiety (2-Mba). After alkaline hydrolysis, the S absolute configuration of 2-Mba was determined by chiral gas chromatography (GC) analysis. In addition, the 11-hydroxytetradecanoic acid moiety (convolvulinolic acid, Con) was suggested by the diagnostic signals of methyl triplet at δ_H 0.85, methylene group at δ_H 2.46 and 2.34, and oxygenated methine at δ_H 3.88. After alkaline and acid hydrolysis, the resulting 11-hydroxytetradecanoic acid showed a fragment ion at m/z 183 $[M - CH_3(CH_2)_2 - H_2O]^+$ by the EIMS data, suggesting the 11-OH group of Con. Its absolute configuration was determined to be S by the Mosher's method.[10]

In the anomeric region, the $^1H–^1H$ COSY data (Fig. 2) indicated five spin systems, which were attributed to three 6-deoxyhexose and two hexose units. The sugars obtained from the acidic hydrolysates were identified as L-rhamnose and D-glucose through the HPLC analysis and their corresponding optical rotations. The β-configurations of D-glucose was determined by a large coupling constant ($J = 7.5$ Hz and 7.6 Hz) for the anomeric protons at δ_H 4.90 and δ_H 5.12 in the ^1H NMR spectrum, while α-configuration of L-rhamnose was revealed by the chemical shift of C-5 of rhamnose (δ_C 69.3, 68.8, 68.5) in the ^{13}C NMR spectrum.[11] The long-range HMBC correlations (Fig. 2) between H-1 of β-Glc (δ_H 4.90) and C-11 (δ_C 82.7) of the 11-hydroxytetradecanoyl moiety indicated that β-Glc was the first hexose unit in the sugar moiety. The sequence of the sugar moiety was determined to be glucosyl-(1 → 3)-[rhamnosyl-(1 → 4)]-rhamnosyl-(1 → 4)-rhamnosyl-(1 → 2)-glucosyl by their long-range HMBC correlations: H-1 of α-Rha (δ_H 5.59) to C-2 of β-Glc (δ_C 82.2), H-1 of α-Rha′ (δ_H 5.85) to C-4 of α-Rha (δ_C 82.2), H-1 of α-Rha″ (δ_H 6.29) to C-4 of α-Rha′ (δ_C 79.3), and δ_H H-1 of β-Glc′ (δ_H 5.12) to C-3 of α-Rha′ (δ_C 80.2). In addition, the positions of esterification, i.e., 2-Mba located at OH-4 of α-Rha″, CA at OH-3 of α-Rha″, Octa at OH-2 of α-Rha′ were inferred from the long-range correlations: H-4 of α-Rha″ (δ_H 6.09) to C-1 of 2-Mba (δ_C 176.3), and H-3 of α-Rha″ (δ_H 5.99) to C-1 of CA (δ_C 166.8), H-2 of α-Rha′ (δ_H 6.34) to C-1 of Octa (δ_C 173.9) respectively. The C-2 (Rha) site of lactonization was corroborated

by the correlation between C-1 of Con (δ_C 173.7) and H-2 of α-Rha (δ_H 6.02). Thus, the structure of compound 1 was identified as (11S)-convolvulinolic acid 11-O-β-D-glucopyranosyl-(1 → 3)-O-[3-O-(trans-cinnamoyl)-4-O-(2S-methylbutanoyl)-α-L-rhamnopyranosyl-(1 → 4)]-O-[2-O-n-octanoyl]-α-L-rhamnopyranosyl-(1 → 4)-O-α-L-rhamnopyranosyl-(1 → 2)-O-β-D-glucopyranoside-(1, 2′-lactone).

The molecular formulas of pharbitins B–E (2–5) were determined as $C_{68}H_{108}O_{27}$, $C_{57}H_{98}O_{26}$, $C_{59}H_{102}O_{26}$ and $C_{64}H_{112}O_{26}$, respectively, based on the ^{13}C NMR (Table 3) and HRESIMS data. The ^1H and ^{13}C NMR spectra indicated that 2–5 consisted of the same complex sugar moiety and (11S)-hydroxytetradecanoyl group as 1. They differed at the kinds of acyl residue and the sites of acylation. The identities of the acyl moieties were determined by LC-HRMS after basic hydrolysis. 2-Mba, CA, Deca (n-decanoic acid) in 2, 2-Mba, Octa in 3, 2-Mba, Deca in 4 and Deca in 5 were identified. The positions of acylation were determined by the HMBC correlations as follows: OH-4 of Rha″ was acylated by 2-Mba in 2–4 and by Deca in 5, OH-2 of Rha′ was acylated by Deca in 2, 4, 5 and by Octa in 3, OH-3 of Rha″ was acylated by CA only in 2. Moreover, the site of lactonization was corroborated as C-2 of Rha according to the correlation between C-1 of Con and H-2 of Rha. Consequently, the structures of 2–5 were determined as shown.

Pharbitin F (6) has the same molecular formula, $C_{66}H_{104}O_{27}$, as 1, according to its HRESIMS data at m/z 1351.6663 $[M + Na]^+$ (calcd 1351.6657). Alkaline hydrolysis of 1 and 6 afforded 2-Mba, CA and Octa in the CHCl$_3$ layer. The sites of acylation of 6 were the same as 1, which was supported by the key HMBC correlation from Rha″ H-4 (δ_H 6.06) to 2-Mba C-1 (δ_C 176.3), Rha″ H-3 (δ_H 5.93) to CA C-1 (δ_C 166.5), Rha′ H-2 (δ_H 6.03) to Octa C-1 (δ_C 173.9). Moreover, ^1H and ^{13}C NMR data of 1 and 6 indicated that they share the same pentasaccharide skeleton. The only difference between 1 and 6 was the position of the lactonization. In the HMBC spectrum of 6, the H-3 proton of Rha resonated at δ_H 5.70 and showed an HMBC correlation to the carbonyl group that resonated at δ_C 175.0 (C-1 of Con),
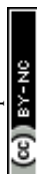
Paper

Table 1 ^{1}H NMR (500 MHz) data of **1–5** (in ppm) (pyridine-d_5)^a

Position	1	2	3	4	5
Glc-1	4.90 d (7.5)	4.91 d (7.4)	4.88 d (7.5)	4.86 d (7.5)	4.89 d (7.4)
2	3.89 m*, ^{b}	3.90 m*	3.87 m*	3.86 m*	3.89 m*
3	4.18 m*	4.19 m*	4.14 m*	4.14 m*	4.17 m*
4	4.12 m*	4.13 m*	4.11 m*	4.10 m*	4.13 m*
5	3.85 m*	3.86 m*	3.83 m*	3.82 m*	3.84 m*
6	4.45 m*, 4.30 dd (11.7, 5.2)	4.46 m*, 4.31 dd (12.2, 5.2)	4.45 m*, 4.30 dd (12.5, 4.0)	4.44m*, 4.28 dd (11.9, 5.5)	4.46m*, 4.32 dd (10.7, 5.1)
Rha-1	5.59 d (1.8)	5.60 d (1.8)	5.58 d (1.8)	5.56 d (1.8)	5.59 d (1.8)
2	6.02 dd (3.4, 1.8)	6.03 dd (3.4, 1.8)	6.02 dd (3.3, 1.8)	6.01 dd (3.3, 1.8)	6.04 dd (3.4, 1.8)
3	5.07 m*	5.07 m*	5.04 m*	5.03 m*	5.03–5.09 m
4	4.16 m*	4.17 m*	4.18 m*	4.17 m*	4.19 m*
5	4.44 m*	4.45 m*	4.43 m*	4.42 m*	4.44 m*
6	1.60 d (6.2)	1.61 d (6.1)	1.60 d (6.2)	1.59 d (6.1)	1.62 d (6.0)
Rha′-1	5.85 d (1.8)	5.86 d (1.9)	5.91 d (1.9)	5.91 d (1.8)	5.94 d (1.9)
2	6.34 br s	6.35 dd (3.2, 1.9)	6.30 dd (3.4, 1.9)	6.29 br s	6.33 dd (3.4, 1.9)
3	4.81 dd (8.9, 3.3)	4.80–4.86 m	4.75–4.81 m	4.74–4.80 m	4.77–4.83 m
4	4.37 m*	4.38 m*	4.34 m*	4.33 m*	4.36 m*
5	4.36 m*	4.37 m*	4.35 m*	4.34 m*	4.37 m*
6	1.65 d (5.7)	1.66 d (5.4)	1.66 d (5.1)	1.64 d (5.5)	1.67 d (5.5)
Rha″-1	6.29 d (1.8)	6.30 d (1.8)	6.24 d (1.9)	6.23 d (1.9)	6.28 d (1.9)
2	5.27 dd (3.1, 1.8)	5.28 br s	4.95 br s	4.94 br s	4.99 m*
3	5.99 dd (9.8, 3.1)	6.00 dd (9.8, 3.1)	4.49–4.57 m	4.51 dd (9.4, 3.8)	4.55–4.61 m
4	6.09 t (9.8)	6.10 t (9.8)	5.76 t (9.4)	5.75 t (9.4)	5.82 t (9.4)
5	4.50 dd (9.8, 6.3)	4.51 dd (9.8, 6.3)	4.36 m*	4.35 m*	4.38 m*
6	1.43 d (6.3)	1.44 d (6.3)	1.40 d (6.2)	1.39 d (6.2)	1.45 d (6.3)
Glc′-1	5.12 d (7.6)	5.13 d (7.6)	5.08 d (7.7)	5.07 d (7.6)	5.11 d (7.6)
2	3.96 m*	3.97 m*	3.96 m*	3.95 m*	3.98 m*
3	4.06 m*	4.07 m*	4.03 m*	4.02 m*	4.05 m*
4	3.93 m*	3.94 m*	3.94 m*	3.93 m*	3.96 m*
5	3.76–3.82 m	3.80 ddd (9.8, 5.9, 2.5)	3.74 ddd (8.9, 5.8, 2.5)	3.73 ddd (8.9, 5.8, 2.5)	3.76 ddd (8.9, 5.9, 2.5)
6	4.40 m*, 4.09 m*	4.41 m*, 4.10 m*	4.38 m*, 4.08 m*	4.37 m*, 4.07 m*	4.41 m*, 4.10 m*
Con-2	2.46 m*, 2.34 m*	2.47 m*, 2.36 m*	2.46 m*, 2.35 m*	2.45 m*, 2.34 m*	2.45 m*, 2.37 m*
11	3.88 m*	3.89 m*	3.86 m*	3.85 m*	3.88 m*
14	0.85 t (6.9)	0.85 t (7.3)	0.85 t (7.3)	0.83 t (7.2)	0.85 t (7.1)
2-Mba-2	2.49 m*	2.50 m*	2.51 m*	2.50 m*	
3	1.70 m*, 1.40 m*	1.71 m*, 1.41 m*	1.78 m*, 1.49 m*	1.77 m*, 1.47 m*	
4	0.82 t (6.9)	0.82 t (7.5)	0.93 t (7.4)	0.92 t (7.4)	
2-Me	1.14 d (6.9)	1.15 d (7.0)	1.20 d (7.0)	1.19 d (7.0)	
CA-2	6.59 d (16.0)	6.59 d (16.0)			
3	7.85 d (16.0)	7.86 d (16.0)			
2′/6′	7.45 2H m	7.46 2H m			
3′/5′	7.34 2H m*	7.34 2H m*			
4′	7.34 m*	7.34 m*			
Octa-2	2.31 m*		2.31 m*		
8	0.79 t (7.0)		0.79 t (6.9)		
Deca-2		2.33 m*		2.30 m*	2.32 m*
10		0.85 t (7.2)		0.83 t (7.2)	0.85 t (7.1)
Deca′-2					2.48 m*
10					0.85 t (7.1)

^{a} Chemical shifts (ppm) referenced to pyridine-d_5 (δ_H 7.58) at 500 MHz. ^{b} Chemical shifts marked with an asterisk (*) indicate overlapped signals.

which suggested the lactone bond was linked at C-3 of Rha in **6** rather than at C-2 of Rha as in **1**. Therefore, the structure of **6** was determined as shown.

Pharbitin G (**7**) has the same molecular formula, $C_{59}H_{102}O_{26}$, as **4**, according to its HRESIMS data at m/z 1249.6550 [M + Na]$^+$ (calcd 1249.6552). 1D NMR and the HMBC spectrum, together with the alkaline hydrolysis analysis, suggested **4** and **7** share the same pentasaccharide skeleton, same acyl functions (2-Mba, Deca) and same sites of acylation (OH-4 of Rha″ was acylated by 2-Mba, OH-2 of Rha′ was acylated by Deca). The only difference between **4** and **7** was the position of the lactonization. The lactonization site was bonded at C-3 of Rha for **7**, while at C-2 of Rha for **4**, on the basis of corresponding HMBC correlation: δ_H 5.68 (Rha H-3) to δ_C 175.0 (Con C-1) in **7**, δ_H 6.01 (Rha H-2) to δ_C 173.7 (Con C-1) in **4**. Thus, the structure of **7** was determined as shown.

Table 2 ^{1}H NMR (500 MHz) data of **6–7** (in ppm) (pyridine-d_5)[a]

Position	6	7
Glc-1	5.04 d (7.8)	5.03 d (8.0)
2	4.28 m*, [b]	4.28 m*, [b]
3	4.37 m*	4.35 m*
4	4.18 m*	4.17 m*
5	3.91 m*	3.91 m*
6	4.56 m*, 4.38 m*	4.50 m*, 4.38 m*
Rha-1	6.47 d (1.8)	6.48 d (1.7)
2	5.24 br s	5.25 br s
3	5.70 dd (10.0, 2.8)	5.68 dd (9.7, 2.7)
4	4.71 m*	4.72 t (9.7)
5	5.07 m*	5.06 m*
6	1.72 d (6.2)	1.70 d (6.1)
Rha'-1	5.63 d (1.8)	5.65 d (1.8)
2	6.03 dd (3.4, 1.8)	6.01 dd (3.5, 1.8)
3	4.74 dd (8.9, 3.4)	4.66 dd (8.8, 3.5)
4	4.37 m*	4.36 m*
5	4.44 m*	4.39 m*
6	1.66 d (5.8)	1.65 d (5.9)
Rha''-1	6.28 d (2.5)	6.22 d (2.0)
2	5.22 br s	4.93 br s
3	5.93 dd (9.8, 2.5)	4.47 m*
4	6.06 t (9.8)	5.75 t (9.7)
5	4.47 m*	4.36 m*
6	1.44 d (6.2)	1.41 d (6.2)
Glc'-1	5.15 d (7.7)	5.10 d (7.6)
2	3.96 m*	3.97 m*
3	4.16 m*	4.14 m*
4	4.18 m*	4.17 m*
5	3.91 m*	3.91 m*
6	4.56 m*, 4.38 m*	4.50 m*, 4.38 m*
Con-2	2.74 ddd (14.2, 10.8, 2.7), 2.32 m*	2.70 ddd (14.2, 10.7, 2.8), 2.28 m*
11	3.94 m*	3.93 m*
14	1.02 t (7.0)	0.95 t (7.1)
Jal-2		
11		
14		
2-Mba-2	2.46 m*	2.50 m*
3	1.69 m*, 1.40 m*	1.77 m*, 1.48 m*
4	0.81 t (7.4)	0.93 t (7.4)
2-Me	1.13 d (7.0)	1.19 d (7.1)
CA-2	6.56 d (16.0)	
3	7.85 d (16.0)	
2'/6'	7.44 2H m	
3'/5'	7.33 2H m*	
4'	7.33 m*	
Octa-2	2.42 m*	
8	0.81 t (6.9)	
Deca-2		2.43 m*
10		0.85 t (7.1)

[a] Chemical shifts (ppm) referenced to pyridine-d_5 (δ_H 7.58) at 500 MHz. [b] Chemical shifts marked with an asterisk (*) indicate overlapped signals.

Isolates (**1–4** and **6**) were examined for their multidrug resistance (MDR) reversal activities in KB/VCR and A549/T cells using the SRB method, while in K562/ADR cell using the MTT method (Tables 4 and S1†). However, only the KB/VCR cell line showed favorable results and as such we proceeded to carry out further experiments with this cell line. The MDR reversal activity in KB/VCR is described below.

The cytotoxicity assay showed that the inhibition ratios of **2** and **4** were less than 50% at 25 μM, indicating that these compounds were noncytotoxic at 25 μM. However, the inhibition ratios of **1**, **3**, **6** were more than 50% at 25 μM, indicating that these compounds were cytotoxic at 25 μM, thus, these compounds were tested at 5 μM. Compounds **2** and **4** enhanced the cytotoxicity of vincristine by 1.1–2.2-fold when incorporated at 25 μM, while compound **1**, **3**, **6** increased the cytotoxicity of vincristine by 0.9–1.3-fold when incorporated at 5 μM. Compound **2** with a CA substituent group at Rha'' C-3 was 2 times more active than compound **4** with no substituent group at the same site. Similar result was observed for compound **1** and **3**, which demonstrated that, substituting Rha'' C-3 with a CA group improves MDR reversal activity.

Moreover, compound **2** was tested for its effects on both P-glycoprotein (P-gp) function and expression (Fig. 3 and 4). Intracellular rhodamine 123 (Rh123)-associated mean fluorescence intensity in KB and KB/VCR cells was used to study the effects of compound on the inhibition of P-gp function. The result showed that the Rh123 accumulation of KB/VCR was a lot less than the parental KB cells and the Rh123 accumulation of KB/VCR pretreated with compound **2** was twice higher than untreated. However, the expression of P-gp detected by Western blot showed that P-gp was overexpressed in KB/VCR cell and compound **2** had no effect on P-gp expression.

Conclusions

The chemical investigation of the seeds of *P. nil* led to the isolation of seven new pentasaccharide resin glycosides pharbitins A–G (**1–7**), and it is the first time resin glycosides with macrolactone rings is being reported from *P. nil*. The isolated resin glycosides shared the same oligosaccharide core, and differed at the kinds of acyl residue, and the sites of acylation. According to the sites of acylation, compounds **1–5** possess 18-membered rings, whereas compounds **6–7** possess 19-membered rings. Compound **2** showed moderate MDR reversal activity in KB/VCR cell, and increased the cytotoxicity of vincristine by 2.2-fold when incorporated at 25 μM. SAR study showed that, substituting Rha'' C-3 with a CA group improves MDR reversal activity. This work therefore contributes to the SAR study of resin glycosides with MDR reversal activities. Furthermore, we found that compound **2** inhibited the function of P-gp but had no effect on P-gp expression.

Experimental

General experimental procedures

Optical rotations were determined with a Perkin Elmer 341 polarimeter. UV spectra were obtained on a Shimadzu UV-2450 spectrophotometer. IR spectra were measured by a Bruker Tensor 27 spectrometer. NMR experiments were recorded in pyridine-d_5 on Bruker AM-400 and Bruker AM-500 spectrometers referenced to solvent peaks (δ_H 7.58; δ_C 135.9). EIMS analyses were performed on a Thermo-DFS mass spectrometer.
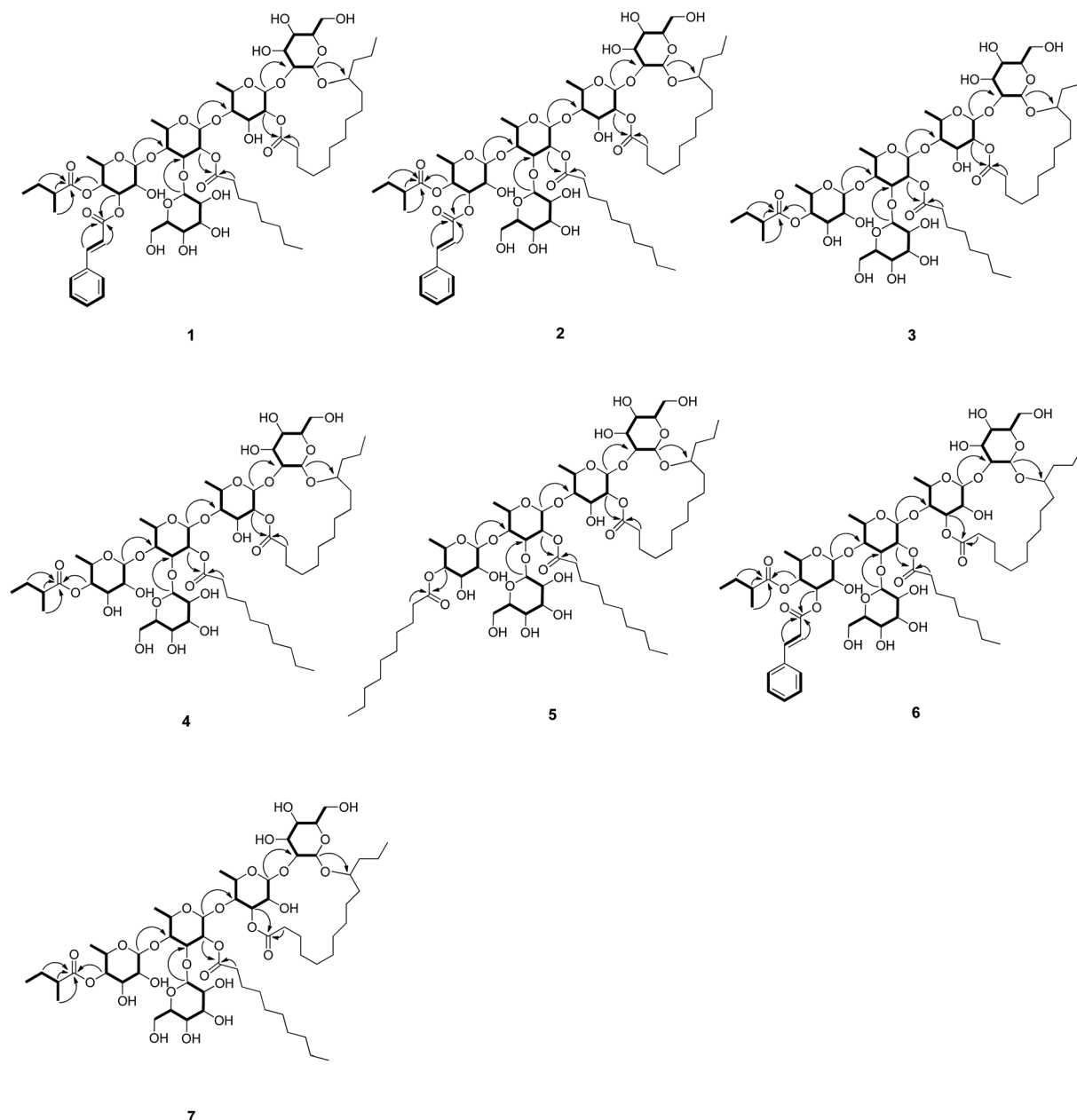
Fig. 2 Key HMBC and ^{1}H–^{1}H COSY correlations of pharbitins A–G (**1–7**).

HRESIMS analyses were performed on an Agilent 6224 TOF mass spectrometer with an ESI interface. Semipreparative HPLC was carried out on an Agilent 1100 series HPLC system with a YMC-Pack ODS-A column (250 × 10 mm, 5 µm). Analytical HPLC was performed on an Agilent 1200 series HPLC system with an Agilent ZORBAX NH$_2$ column (150 × 4.6 mm, 5 µm). Silica gel (200–300 mesh, Qingdao Haiyang Chemical Co. Ltd., People's Republic of China), C$_{18}$ reversed-phase (RP-18) silica gel (20–45 µm; Fuji Silysia Chemical Ltd., Japan) and Sephadex LH-20 gel (Amersham Biosciences, Sweden) were used for column chromatography (CC). Pre-coated silica gel GF254 plates (Qingdao Haiyang Chemical Co. Ltd., People's Republic of China) were used for TLC.

Plant material

Seeds of *Pharbitis nil* were collected in Guangxi, China, in August 2013 and identified by Prof. Heming Yang. A voucher specimen (no. SIMM810) was deposited at the Herbarium of the Shanghai Institute of Materia Medica, Chinese Academy of Sciences and People's Republic of China.

Extraction and isolation

Air–dried, powdered seeds of *Pharbitis nil* (5.0 kg) were refluxed with 95% EtOH three times and concentrated *in vacuo* to give a crude extract (230 g), which was suspended in 2 L of water and then extracted with EtOAc to give the EtOAc-soluble fraction (168 g). The EtOAc layer was concentrated, and subjected to

Table 3 ^{13}C NMR (125 MHz) data of **1–7** (in ppm) (pyridine-d_5)[a]

Position	1	2	3	4	5	6	7
Glc-1	104.6	104.6	104.6	104.6	104.7	101.7	101.7
2	82.2	82.3	82.3	82.3	82.3	75.6	75.8
3	76.9	76.9	76.9	76.9	77.0	79.9	79.7
4	72.0	72.0	72.2	72.1	72.2	72.2	72.4
5	78.3	78.4	78.3	78.2	78.4	78.4	78.5
6	63.1	63.2	63.2	63.1	63.2	63.1	63.2
Rha-1	98.8	98.8	98.9	98.8	98.9	100.3	100.5
2	73.8	73.9	73.9	73.9	73.9	70.2	70.2
3	69.6	69.7	69.8	69.7	69.8	78.1	78.3
4	82.2	82.2	81.6	81.6	81.5	77.7	77.1
5	69.3	69.4	69.3	69.3	69.4	68.5	68.5
6	19.3	19.4	19.2	19.2	19.3	19.6	19.6
Rha′-1	100.5	100.6	100.3	100.2	100.3	99.8	99.7
2	73.6	73.6	73.5	73.4	73.5	72.6	72.5
3	80.2	80.3	80.5	80.4	80.6	80.5	80.7
4	79.3	79.3	79.0	78.9	78.9	79.4	78.9
5	68.8	68.8	68.8	68.8	68.9	68.5	68.6
6	19.4	19.4	19.5	19.4	19.5	19.2	19.1
Rha″-1	103.7	103.7	103.6	103.5	103.6	103.7	103.8
2	70.2	70.3	72.8	72.8	72.8	70.2	72.7
3	73.3	73.4	70.7	70.6	70.7	73.2	70.6
4	72.2	72.2	75.5	75.5	75.9	72.4	75.6
5	68.5	68.5	68.5	68.5	68.6	68.5	68.5
6	18.2	18.3	18.4	18.3	18.4	18.3	18.4
Glc′-1	105.8	105.9	105.8	105.7	105.8	105.1	105.2
2	75.5	75.6	75.6	75.5	75.6	75.9	75.6
3	78.8	78.8	78.8	78.7	78.9	78.8	78.6
4	71.8	71.9	71.8	71.7	71.8	71.2	71.1
5	78.4	78.5	78.5	78.4	78.6	78.5	78.8
6	63.3	63.3	63.3	63.2	63.3	62.9	62.9
Con-1	173.7	173.7	173.7	173.7	173.7	175.0	175.0
2	34.6	34.6	34.6	34.6	34.6	34.5	34.5
11	82.7	82.7	82.7	82.7	82.8	79.8	80.0
14	14.9	14.9	14.9	14.8	14.9	15.2	15.1
2-Mba-1	176.3	176.3	176.7	176.6		176.3	176.7
2	41.9	41.9	41.9	41.9		41.9	41.9
3	27.3	27.4	27.5	27.4		27.3	27.4
4	12.1	12.2	12.1	12.1		12.1	12.1
5	17.3	17.3	17.4	17.3		17.2	17.4
CA-1	166.8	166.8				166.5	
2	118.9	118.9				119.0	
3	145.7	145.7				145.6	
1′	135.1	135.1				135.1	
2′/6′	128.8	128.9				128.8	
3′/5′	129.6	129.6				129.6	
4′	131.1	131.1				131.0	
Octa-1	173.9		174.0			173.9	
2	34.9		34.9			34.8	
8	14.6		14.6			14.6	
Deca-1		173.9		174.0	174.0		174.0
2		34.9		34.9	34.9		34.9
10		14.6		14.6	14.7		14.7
Deca′-1					173.9		
2					35.1		
10					14.7		

[a] Chemical shifts (ppm) referenced to pyridine-d_5 (δ_C 135.9) at 125 MHz.

silica gel CC, eluting with petroleum ether/acetone in a gradient manner (100 : 0 to 0 : 100, v/v) to afford nine fractions (A-I). Fraction G was subjected to silica gel CC and eluted with CHCl$_3$/MeOH (20 : 1 to 1 : 1) to yield subfractions (G1–G7).

Fraction G3 was further subjected to a Sephadex LH-20 gel column followed by a RP-C18 column using a gradient of MeOH/H$_2$O (80 : 20 to 100 : 0, v/v) to give **6** (12 mg). Fraction H was applied to silica gel CC and eluted with CHCl$_3$/MeOH (20 : 1

Table 4 Results of modulating MDR[a] Activities in KB/VCR cells of compounds 1–4 and 6

Sample	Inhibition ratio % (25 μM)	Vincristine + Sample[b]	
		IC$_{50}$ value (μM)	RF[c] value
2	5.62	0.22	2.2
4	4.17	0.44	1.1
Vincristine		0.48	

Sample	Inhibition ratio % (5 μM)	Vincristine + Sample[d]	
		IC$_{50}$ value (μM)	RF[e] value
1	2.84	0.36	1.3
3	1.85	0.53	0.9
6	10.64	0.37	1.3
Vincristine		0.48	

[a] MDR: multidrug resistance. [b] Serial dilutions ranging from 0.125 to 1 μM of vincristine in the presence or absence of 25 μM sample. [c] RF: IC$_{50}$ of VCR alone/IC$_{50}$ of VCR in presence of 25 μM sample. [d] Serial dilutions ranging from 0.125 to 1 μM of vincristine in the presence or absence of 5 μM sample. [e] RF: IC$_{50}$ of VCR alone/IC$_{50}$ of VCR in presence of 5 μM sample.
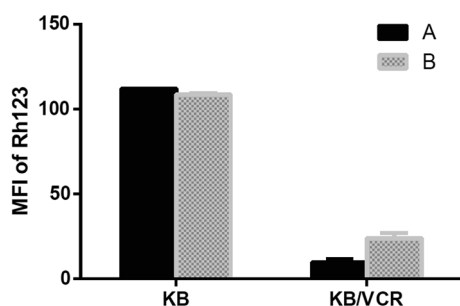
Fig. 3 Effects of compound 2 on Rh123 accumulation in drug-sensitive KB and multidrug-resistant KB/VCR cells. Cells were respectively untreated (A) and pretreated with 25 μM of compound 2 (B).
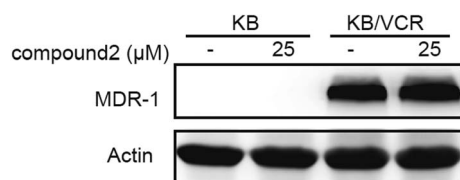
Fig. 4 Effects of compound 2 on MDR-1 protein expression in drug-sensitive KB and multidrug-resistant KB/VCR cells. Cells were treated with compound 2 and MDR-1 protein expression was analyzed by Western blot.

to 1 : 1) to afford subfractions (H1–H6). Fraction H2 was further purified by a Sephadex LH-20 gel column followed by preparative HPLC (MeOH/H$_2$O, 100 : 0, v/v) to obtain 1 (60 mg) and 2 (60 mg). Fraction H3 was chromatographed on a Sephadex LH-20 gel column followed by a RP-C18 column using a gradient of MeOH/H$_2$O (80 : 20 to 100 : 0, v/v) to yield 7 (8 mg). Same

method was applied to fraction H4 to yield compound 5 (10 mg). Fraction H5 was subjected to a RP-C18 column (50 : 50 to 100 : 0, v/v) to give five subfractions (H5A-H5E). Fraction H5D was chromatographed on a silica gel column and eluted with CHCl$_3$/MeOH (10 : 1 to 5 : 1) to give fraction H5D1 and H5D2, which were further purified on an open ODS column (MeOH/H$_2$O, 85 : 15 to 100 : 0, v/v) to obtain 3 (60 mg) and 4 (60 mg), respectively.

Pharbitin A (1). Colorless gum; $[\alpha]_D^{26}$ −29.5 (c 0.1, MeOH); UV (MeOH) λ_{max} (log ε) 203 (3.89), 217 (3.91), 280 (4.09) nm; IR (KBr) ν_{max} 3426, 2926, 2855, 1724, 1635, 1052 cm^{-1}; ^{1}H and ^{13}C NMR data, see Tables 1 and 3; HRESIMS m/z 1351.6647 [M + Na]$^+$ (calcd for C$_{66}$H$_{104}$O$_{27}$Na, 1351.6657).

Pharbitin B (2). Colorless gum; $[\alpha]_D^{26}$ −33.0 (c 0.1, MeOH); UV (MeOH) λ_{max} (log ε) 203 (3.66), 217 (3.64), 279 (3.80) nm; IR (KBr) ν_{max} 3429, 2929, 2858, 1730, 1632, 1049 cm^{-1}; ^{1}H and ^{13}C NMR data, see Tables 1 and 3; HRESIMS m/z 1379.6988 [M + Na]$^+$ (calcd for C$_{68}$H$_{108}$O$_{27}$Na, 1379.6970).

Pharbitin C (3). Colorless gum; $[\alpha]_D^{26}$ −23.7 (c 0.1, MeOH); UV (MeOH) λ_{max} (log ε) 203 (3.64), 275 (2.45) nm; IR (KBr) ν_{max} 3405, 2929, 2852, 1727, 1046 cm^{-1}; ^{1}H and ^{13}C NMR data, see Tables 1 and 3; HRESIMS m/z 1221.6258 [M + Na]$^+$ (calcd for C$_{57}$H$_{98}$O$_{26}$Na, 1221.6239).

Pharbitin D (4). Colorless gum; $[\alpha]_D^{27}$ −29.8 (c 0.1, MeOH); UV (MeOH) λ_{max} (log ε) 203 (3.59), 275 (2.43) nm; IR (KBr) ν_{max} 3417, 2926, 2855, 1727, 1052 cm^{-1}; ^{1}H and ^{13}C NMR data, see Tables 1 and 3; HRESIMS m/z 1249.6561 [M + Na]$^+$ (calcd for C$_{59}$H$_{102}$O$_{26}$Na, 1249.6552).

Pharbitin E (5). Colorless gum; $[\alpha]_D^{27}$ −35.0 (c 0.1, MeOH); UV (MeOH) λ_{max} (log ε) 203 (3.43), 275 (2.38) nm; IR (KBr) ν_{max} 3396, 2926, 2855, 1727, 1046 cm^{-1}; ^{1}H and ^{13}C NMR data, see Tables 1 and 3; HRESIMS m/z 1277.6862 [M + Na]$^+$ (calcd for C$_{61}$H$_{106}$O$_{26}$Na, 1277.6865).

Pharbitin F (6). Colorless gum; $[\alpha]_D^{25}$ −35.0 (c 0.1, MeOH); UV (MeOH) λ_{max} (log ε) 203 (3.83), 217 (3.85), 280 (4.05) nm; IR (KBr) ν_{max} 3417, 2926, 2861, 1730, 1635, 1043 cm^{-1}; ^{1}H and ^{13}C NMR data, see Tables 2 and 3; HRESIMS m/z 1351.6663 [M + Na]$^+$ (calcd for C$_{66}$H$_{104}$O$_{27}$Na, 1351.6657).

Pharbitin G (7). Colorless gum; $[\alpha]_D^{26}$ −48.0 (c 0.1, MeOH); UV (MeOH) λ_{max} (log ε) 203 (3.57), 275 (2.66) nm; IR (KBr) ν_{max} 3399, 2926, 2855, 1727, 1049 cm^{-1}; ^{1}H and ^{13}C NMR data, see Tables 2 and 3; HRESIMS m/z 1249.6550 [M + Na]$^+$ (calcd for C$_{59}$H$_{102}$O$_{26}$Na, 1249.6552).

Aglycon identification

Compounds 1–7 (5 mg, each) were separately dissolved in 5% NaOH (4 mL) and refluxed at 90 °C for 4 h. Each of the reaction mixtures were acidified to PH 4, followed by extraction with CHCl$_3$ (3 × 4 mL) and concentration.[12] The CHCl$_3$ layer was then analyzed by HRESIMS to identify organic acids: 2-methyl-butanoic acid (m/z 101.0606 [M − H]$^-$, calcd 101.0608) in 1–4 and 6–7; n-octanoic acid (m/z 143.1080 [M − H]$^-$, calcd 143.1078) in 1, 3 and 6; n-decanoic acid (m/z 171.1390 [M − H]$^-$, calcd 171.1391) in 2, 4, 5 and 7; trans-cinnamic acid (m/z 147.0453 [M − H]$^-$, calcd 147.0452) in 1, 2 and 6. The CHCl$_3$ layer was also analyzed by chiral GC to determined the absolute

configuration of 2-methylbutanoic acid. In addition, the aqueous phase *via* $CHCl_3$ extraction was then extracted with *n*-BuOH (3 × 4 mL) and concentrated to yield a colorless solid. The residue in 1 N H_2SO_4 (4 mL) was refluxed at 90 °C for 4 h. The reaction mixture was extracted with $CHCl_3$ (3 × 4 mL), which was further concentrated and purified to afford 11-hydroxytetradecanoic acid in **1–7**. The 11-hydroxytetradecanoic acid was further separately treated with (*S*)-MPTA chloride and (*R*)-MPTA chloride in pyridine-d_5, and allowed to stand for 12 h at room temperature. The *S* configuration of 11-hydroxytetradecanoic acid was determined by the chemical shift difference ($\Delta\delta = \delta_S - \delta_R$, $\Delta\delta_{\text{H-14}} = -0.067$).

(11S)-Hydroxytetradecanoic acid. EIMS *m/z* [M − $CH_3(CH_2)_2$ − H_2O]$^+$ 183 (100), 143 (21), 129 (32), 95 (35), 81 (34), 73 (38), 69 (41), 57 (29), 55 (77); HRESIMS *m/z* 267.1930 [M + Na]$^+$ (calcd for $C_{14}H_{28}O_3Na$, 267.1931).

11-(S-MPTA)-hydroxytetradecanoic acid. ^{1}H NMR (in pyridine-d_5, 400 MHz) δ 0.789 (3H, t, *J* = 7.3 Hz, Me-14), 5.266 (1H, m, H-11), 2.523 (2H, t, *J* = 7.0 Hz, H-2).

11-(R-MPTA)-hydroxytetradecanoic acid. ^{1}H NMR (in pyridine-d_5, 400 MHz) δ 0.856 (3H, t, *J* = 7.3 Hz, Me-14), 5.264 (1H, m, H-11), 2.522 (2H, t, *J* = 7.0 Hz, H-2).

Sugar analysis

Compound **1** (20.0 mg) was hydrolyzed by alkali and acid, as described in the aglycone identification section. The aqueous phase was extracted with *n*-BuOH (3 × 4 mL) after acid hydrolysis and concentrated to yield a colorless solid. The residue was dissolved in H_2O and directly analyzed by HPLC with authentic samples (MeCN–H_2O, 90/10): D-glucose eluted at 11.9 min, L-rhamnose at 5.2 min. Each of these eluates was individually collected, concentrated, and dissolved in H_2O. The elutes were identified as D-glucose $[\alpha]_D^{21}$ +54.7 (*c* 0.1, H_2O), L-rhamnose $[\alpha]_D^{21}$ +8.7 (*c* 0.1, H_2O) through comparisons of their specific rotations with those of the corresponding authentic samples.

MDR reversal assays

SRB assay. The MDR reversal activities of the test compounds against the KB/VCR (Zhongshan School of Medicine) and A549/T (KeyGEN BioTECH) cells were measured using a sulforhodamine B (SRB) assay. Briefly, cells were plated in 96-well culture plates for 24 h and treated with serial dilutions of vincristine (Sigma) ranging from 0.125 to 1 μM and taxel (Selleck) ranging from 0.6 to 20 μM, with or without 25 μM of the samples. After incubation for 72 h under a humidified atmosphere of 5% CO_2 at 37 °C, KB/VCR and A549T cells were fixed with 10% trichloroacetic acid and incubated at 4 °C for 1 h. After washing with distilled H_2O and air drying, the plates were stained for 15 min with 100 μL of 0.4% SRB in 1% glacial HOAc. The plates were washed with 1% HOAc and air dried. For reading of the plates, the protein-bound dye was dissolved in 150 μL of 10 mM Tris base. The absorbance was measured at 510 nm on a microplate spectrophotometer (Molecular Devices SpectraMax 340, Sunnyvale, CA, USA).

MTT assay. The MDR reversal activities of the test compounds against the K562/ADR (KeyGEN BioTECH) cells were measured using a MTT assay. Briefly, cells were plated in 96-well culture plates for 24 h and treated with serial dilutions of adriamycin (Selleck) ranging from 3.1 to 100 μM. Then cells were added 10 μL 0.5 mg mL^{-1} MTT and incubated for 4 h. At last, DMSO was added followed by detection of the absorbance value at a wavelength of 570 nm.

The results were expressed as IC_{50} values. The reversal fold (RF) as potency of reversal was obtained from fitting the data to RF = IC_{50} of vincristine or taxel or adriamycin alone/IC_{50} of vincristine or taxel or adriamycin in the presence of sample.[13]

Intracellular Rh123 accumulation assay. KB and KB/VCR cells were seeded in six-well plates at a 1 × 10^6 cells density and cultured for 24 h. Then fresh media containing 2.5 μg mL^{-1} of Rh123 (Sigma) and 2.5 μM of compound **2** were added and incubated for 30 min. At the end of the time, the accumulation of Rh123 was stopped by washing with ice-cold PBS. Cells were harvested and the intracellular mean fluorescence intensity (MFI) associated with Rh123 was measured with a FACS calibur cytometer (Ex at 485 nm Em^{-1} at 530 nm) data analysis was performed using FlowJo.

P-gp expression assay. To identify the P-gp protein expression, the total protein level was measured by western blot. Cells were seeded 1 × 10^6 per well in six-plates and cultured overnight. The cells were treated with 25 μM compound **2** for 30 min, and then harvested for western blot analysis.

Conflicts of interest

There are no conflicts to declare.

Acknowledgements

References

1 R. Pereda-Miranda, R. Villatoro-Vera, M. Bah and A. Lorence, *Rev. Latinoam. Quim.*, 2009, **37**, 144–154.

2 L. Chérigo, R. Pereda-Miranda, M. Fragoso-Serrano, N. Jacobo-Herrera, G. Kaatz and S. Gibbons, *J. Nat. Prod.*, 2008, **71**, 1037–1045.

3 G. Figueroa-Gonzál, N. Jacobo-Herrera, A. Zentella-Dehesa and R. Pereda-Miranda, *J. Nat. Prod.*, 2012, **75**, 93–97.

4 I. Kitagawa, K. Ohashi, H. Kawanishi, H. Shibiya, K. Shinkai and H. Akedo, *Chem. Pharm. Bull.*, 1989, **37**, 1679–1681.

5 W. Q. Wang, W. B. Song, X. J. Lan, M. Huang and L. J. Xuan, *J. Nat. Prod.*, 2014, **77**, 2234–2240.

6 M. One, N. Noda, T. Kawasaki and K. Miyahara, *Chem. Pharm. Bull.*, 1990, **38**, 1892–1897.

7 T. Kawasaki, H. Okabe and I. Nakatsuka, *Chem. Pharm. Bull.*, 1971, **19**, 1144–1149.

8 H. Okabe and T. Kawasaki, *Chem. Pharm. Bull.*, 1972, **20**, 514–520.

9 Y. Q. Yin, J. S. Wang, J. G. Luo and L. Y. Kong, *Carbohydr. Res.*, 2009, **344**, 466–473.

10 B. W. Yu, J. G. Luo, J. S. Wang, D. M. Zhang, S. S. Yu and L. Y. Kong, *J. Nat. Prod.*, 2011, **74**, 620–628.

11 S. M. Sang, A. N. Lao, Y. Leng, Z. P. Gu, Z. L. Chen, J. Uzawa and Y. Fji-moto, *Tetrahedron Lett.*, 2000, **41**, 9205–9208.

12 B. Y. Fan, Y. C. Gu, Y. He, Z. R. Li, J. G. Luo and L. Y. Kong, *J. Nat. Prod.*, 2014, **77**, 2264–2272.

13 B. S. Ji, L. He and G. Q. Liu, *Life Sci.*, 2005, **77**, 2221–2232.